Hydrol. Earth Syst. Sci. Discuss., 5, 2951–2973, 2008
www.hydrol-earth-syst-sci-discuss.net/5/2951/2008/

Hydrology and Earth System Sciences Discussions

Papers published in *Hydrology and Earth System Sciences Discussions* are under open-access review for the journal *Hydrology and Earth System Sciences*

Improved estimation of flood parameters by combining space based SAR data with very high resolution digital elevation data

H. Zwenzner and S. Voigt

German Remote Sensing Data Center, German Aerospace Center, Oberpfaffenhofen, Germany

Received: 12 September 2008 – Accepted: 12 September 2008 – Published: 29 October 2008

Correspondence to: H. Zwenzner (hendrik.zwenzner@dlr.de)

Published by Copernicus Publications on behalf of the European Geosciences Union.

Abstract

Severe flood events turned out to be the most devastating catastrophes for Europe's population, economy and environment during the past decades. The total loss caused by the August 2002 flood is estimated to be 10 billion Euros for Germany alone. Due to their capability to present a synoptic view of the spatial extent of floods, remote sensing technology, and especially synthetic aperture radar (SAR) systems, have been successfully applied for flood mapping and monitoring applications. However, the quality and accuracy of the flood masks and derived flood parameters always depends on the scale and the geometric precision of the original data as well as on the classification accuracy of the derived data products. The incorporation of auxiliary information such as elevation data can help to improve the plausibility and reliability of the derived flood masks as well as higher level products. This paper presents methods to improve the matching of flood masks with very high resolution digital elevation models as derived from LiDAR measurements for example. In the following, a cross section approach is presented that allows the dynamic fitting of the position of flood mask profiles according to the underlying terrain information from the DEM. This approach is tested in two study areas, using different input data sets. The first test area is part of the Elbe River (Germany) where flood masks derived from Radarsat-1 and IKONOS during the 2002 flood are used in combination with a LiDAR DEM of 1 m spatial resolution. The other test data set is located on the River Severn (UK) and flood masks derived from the TerraSAR-X satellite and aerial photos acquired during the 2007 flood are used in combination with a LiDAR DEM of 2 m pixel spacing. By means of these two examples the performance of the matching technique and the scaling effects are analysed and discussed. Furthermore, the systematic flood mapping capability of the different imaging systems are examined. It could be shown that the combination of high resolution SAR data and LiDAR DEM allows the derivation of higher level flood parameters such as flood depth estimates, as presented for the Severn area. Finally, the potential and the constraints of the approach are evaluated and discussed.

1 Introduction

Mapping of large scale flood events is not only of major concern for disaster response teams and flood management officials but also poses a key task to hydrologists and the industry in order to generate reference data and calibration information for dynamic flood models, damage estimates, flood plain mapping tasks and further applications. This applies for gauged basins, where gauges may fail or where flooded areas cannot be characterised sufficiently by the gauge data alone, and it applies even more for ungauged basins, where often only little information on the flood dynamics and basin response to extreme events is available. During the past decades airborne and spaceborne remote sensing platforms have been frequently used to map and monitor flood extent in all kinds of basins (Horritt et al., 2003; Sanyal and Lu, 2004; Wang, 2004; Schneiderhan et al., 2007). However, in many cases flood extent alone is not sufficient to characterise a given flood situation adequately. Often parameters like inundation depth or duration of a specific flood situation are required, e.g. as input for damage models (Thieken et al., 2005). As different remote sensing sensors have different ground resolution and varying flood/water detection potential, it is important to be aware of such limitations when processing the respective flood masks in GIS operations or when generating flood maps. This is the case when flood masks are combined with digital elevation data to derive spatially distributed estimates of inundation depths or to exactly locate the land-water boundary in a digital terrain model (Sanders, 2007; Ling et al., 2008). In such cases even small geometric inaccuracies during the geocoding process or slight classification errors (local or general in character) can significantly reduce the quality of higher level products such as inundation depths.

In order to enhance the geometric and thematic reliability of flood masks derived by remote sensing techniques, we here present methods to improve the matching of flood masks with very high resolution digital elevation models as derived from LiDAR measurements (Fowler, 2002). By applying these matching techniques, the hydrological plausibility and reliability of flood masks is improved, so that further processing in

HESSD
5, 2951–2973, 2008

hydrological or hydraulic models can be performed with sufficient accuracy. This is of particular relevance whenever applying remote sensing techniques to operational flood monitoring or for rapid mapping purposes, i.e. when the processing and verification of the results have to be achieved under time pressure. Only a few authors have presented techniques to establish such links of remotely sensed flood masks with high resolution digital elevation data sets. Matgen et al. (2007) tested and compared methods for flood depth interpolation based on flood masks derived from SAR imagery. Bates et al. (2006) used a 2-D hydraulic model approach to cross-compare the results with SAR derived flood extent maps, while Meinel et al. (2003) presented concepts for computing water levels using elevation readings from intersecting IKONOS flood masks with LiDAR DEMs and terrestrial land/water line observations. Schumann et al. (2007) used different regression models to fit the left and right bank elevation readings from SAR based water mask / DEM intersections. All authors described the difficulty of precisely combing water masks and DEMs, as geometric errors and thematic classification errors in the remote sensing data remain high. The methods presented in this paper seek to reduce such residual errors through local matching operations.

2 Methodological approach

The technique presented here is based on the concept of locally fitting a carefully processed flood mask into high resolution digital elevation data sets. The approach is based on the assumption that small geometric or thematic processing errors can be compensated by the fitting process and the hydraulic accuracy can be improved through these fitting operations. The matching process can only be carried out in certain ranges, as the approach is neither meant to inter- or extrapolate flood masks nor to substitute accurate hydraulic approaches. The character of the digital elevation data is of key relevance to this approach, as remaining artefacts like vegetation, removable objects or interpolation errors in the DEM have an influence on the matching result (Fowler, 2002).

The matching concept is based on densely spaced profiles located orthogonally along the main river flow line. Ideally, this line should be the centreline of the area of the flood water body given by the flood mask rather than the centreline of the normal water body. Especially for large flood situations, when the water flow takes a different path than at normal water level, the centreline should represent the effective flood situation. In other cases the mean water flow direction can be used as a centreline for the set up of the cross section profiles. In order to avoid too much overlap between the cross sections, the sinuosity of centreline should remain low. The distance between cross sections as well as the sampling distance within profiles depends on the geometric resolution of the remote sensing data from which the water mask was derived.

The cross sections are set up as profiles of the river basin topography which turns into bathymetry once the river is flooded. Once the respective river section is characterised by these profiles they can be used for intersection with the flood. Each profile segment which is labelled as "flooded" is then checked for its hydraulic plausibility. This means that segments with a mean elevation above a certain threshold are excluded from the overall flood profile. Assuming a planar water level orthogonally to the flow direction, the elevation reading of the left border is compared to the elevation of the right border for the remaining cross section profile. Differences are balanced by shifting the flood profile horizontally along the cross section to find the position of the lowest flood profile elevation. This is done by using a moving window over a defined range of sampling points. Theoretically, this step provides the possibility to compensate for a systematic geometric displacement of the remote sensing data on the basis of the elevation model.

For the resulting position, the elevation of the water level is calculated from the elevation of the left and right border of the flood profile. This is done for each individual cross section along the river flow line in order to establish a longitudinal profile of the flood level. A moving average is applied to the longitudinal water level to obtain a smooth water surface which serves as reference water level for the flood depth delineation. The

horizontal extent of the cross section flood profiles is then adjusted according to the reference water level and the flood plain topography. Thereby, thematic classification errors which occurred during the water mask generation can be compensated.

Each profile is stored in a database and all intersections, cross-checking and matching operations can be computed independently. Hence, even large data sets can be handled quite easily and the precomputed profile database can be used for a wide range of flood situations as they occur. When using the aforementioned parameters the approach works well in river basins with pronounced terrain. It is supposed to be less efficient in flat and extensive flood plains; however, it has not been tested in such areas yet.

3 Case study on River Elbe, Germany

3.1 Study area and flood situation

The extreme flood event in August 2002 affected a number of rivers in Central Europe and especially the Elbe. Due to all-time high summer rainfall amounts and intensities in the headwaters and tributaries of the Elbe River, the water gauge at the city centre of Dresden measured a record water level of 9.4 m on 17 August 2002. This flood level exceeded the last recorded all-time flood peak of the year 1845 by 63 cm.

Figure 1 gives an overview of the study area which comprises a section of the middle course of the Elbe River of about 15 km length. The heavily flooded city centre of Dresden is located about 20 km upstream, southeast of the study area. The floodplain geomorphology exhibits pronounced terrain with some steep slopes adjacent to the water course. The gradient in flow direction is about 7 m for this river section which provokes a straight river flow.

3.2 Data sets and pre-processing

A Radarsat-1 scene showing the flood situation of the Elbe River on 18 August 2002, one day after the flood peak, was used for this study. First of all, the raw satellite data were processed and geocoded. The pixel spacing of the resulting image was 12.5 m. An adaptive Lee-Sigma filtering with a window size of 7×7 pixels was then applied on the SAR data in order to reduce speckle and to support homogeneous water classification. A binary flood mask was derived using a pixel-based threshold classification approach (Brivio et al., 2002). The assumption of the threshold classification approach is that all pixels with backscatter intensities below a certain threshold are classified as "flooded" whereas pixels above the threshold are classified as "non-flooded". Fine tuning of the threshold was done by trial and error procedures, to find the appropriate threshold that comprises all areas with low backscatter, assuming to be water within the flood plain, and simultaneously not capturing too many non-flooded areas. As a final step of the classification small islands and lakes were removed.

A LiDAR DEM of the Elbe flood plain with 1 metre horizontal resolution and a vertical accuracy of 0.1 m was available for the study area. For validation and cross-comparison an optical IKONOS satellite image with four channels and 1 m resolution, acquired three hours after the Radarsat-1 scene, was used. The IKONOS scene was orthorectified and visually interpreted. Because of its high spatial resolution and the good perceptibility of the flooded area, especially in the near infrared channel, a detailed flood mask could be digitised. This flood mask is assumed to reliably reflect the real flood situation.

3.3 Case specific analysis

As indicated in Fig. 1, the flood mask derived from Radarsat-1 data shows large differences in flood extent when compared to the flood mask inferred from IKONOS imagery. According to the geometric resolution of the Radarsat-1 data, cross section flood profiles were generated at intervals of 100 m along the water course of the mean water

level (see Fig. 4). The sampling distance along the profiles was 10 m. It can be recognised from Fig. 1 that the Radarsat-1 flood mask partially includes areas on the hill slopes of the left river bank which were misclassified because of low backscatter intensities resulting from radar shadow. Obviously misclassified profile segments and segments not connected to the main flood surface were excluded from further processing. By applying the profile matching methodology described in Sect. 2, all valid profile segments were shifted horizontally and adjusted to the flood plain topography. Figure 2 shows a comparison of the elevation of the left and right boundary of the flood profiles in flow direction, before and after the shifting was performed.

The same method and cross section profiles were applied on the flood mask derived from IKONOS imagery. Figure 3 presents a comparison of the water level readings derived from Radarsat-1 and IKONOS for each individual profile along the river reach.

3.4 Results

Large outliers in the elevation of the left land-water boundary, which were caused by classification errors due to radar shadow could be eliminated by applying the profile shifting method (see Fig. 2). As a result the given flood profiles from Radarsat-1 could be corrected and proved to be hydraulically plausible. This is confirmed by Fig. 4, which shows that all shifted flood profiles lie within the IKONOS flood mask. However, the derived water levels from the terrain-adjusted flood profiles indicate a large underestimation of flood levels when compared to water levels from IKONOS (see Fig. 3). Generally, the elevation of the flood surface derived from the Radarsat-1 profiles is highly variable. A number of flood profiles present a water level similar to the normal water level. Since flooded area and water level are closely correlated, it follows that the flooded area detected by Radarsat-1 at these cross sections is underestimated and the profiles can be considered as too short. Thematic classification errors due to flooded vegetation or objects which caused high backscatter intensities can be regarded as the main reasons for these inaccuracies. As indicated by the regression lines in Fig. 3, the water levels derived from Radarsat-1 profiles are underestimated by more than two

metres compared to water levels derived from IKONOS flood masks. This leads to the conclusion that for this specific situation the reliability of the Radarsat-1 flood masks can not be guaranteed to yield reasonable estimates of flood depth.

4 Application for high resolution SAR data at River Severn, UK

4.1 Study area and flood situation

The severe flood situation on the River Severn occurred during the summer season and was induced by heavy and enduring rainfall over the Gloucestershire Region in Southeast England. The record flood level at Tewkesbury was measured 5.43 m on 22 July 2007 which was 13 cm above the last highest record from the year 1947. A number of water gauges did not operate regularly in terms of a continuous flood monitoring. However, the flood situation was stable over several days with two local maxima, the first induced by surface water from local precipitation that could not drain away quickly and the latter induced by rising water levels originating from upstream rainfall.

The study area presented in Fig. 5 comprises a section of the River Severn of about 8 km length including the confluence of the River Avon coming from northeast. The heavily flooded city of Tewkesbury is located east of the confluence and can be seen in the TerraSAR-X image as bright areas with high backscatter intensity (see Fig. 5). The study area is part of the lower course of the River Severn, and opposed to the Elbe River, the terrain is relatively flat with a very gentle gradient in flow direction which hampers flood water to drain away quickly.

4.2 Data sets and pre-processing

This case study is based on a TerraSAR-X StripMap scene with 3 m pixel spacing showing the flood situation on 25 July 2007. In order to reduce speckle and obtain homogeneous water classifications as well as to remove small islands in the data, an

adaptive Lee-Sigma filter with a window size of 31×31 pixels was applied to the image. In contrast to the Elbe case study and the Radarsat-1 pre-processing, a multiresolution segmentation was conducted on the high resolution TerraSAR-X data (Blaschke et al., 2000; Baatz and Schäpe, 2000).

Afterwards, a semi-automatic threshold classification approach was applied to the dataset. Small gaps were filled and adjoining ambiguous segments were added to reliably classified flooded segments by using neighbourhood functions. Finally, a binary flood mask with 3 m resolution was derived.

A LiDAR-DEM with a horizontal resolution of 2 m and a vertical accuracy of 0.1 m was used for this study. For validation and cross checking purposes, orthorectified aerial photographs acquired 15 h prior to the TerraSAR-X overpass could be obtained. Similarly to the IKONOS satellite imagery, the aerial photos were visually interpreted and a flood mask was derived by manual digitisation.

4.3 Case specific analysis

Corresponding to the higher resolution of the TerraSAR-X flood mask, cross section flood profiles were generated at intervals of 50 m between profiles and a sampling distance of 5 m along the profiles. As illustrated in Fig. 5, the cross section profiles were arranged orthogonally to a centreline which was digitised through the flood shape in flow direction.

The profile matching method described in Sect. 2 was applied to the flood profiles derived from the TerraSAR-X flood mask and the optimal position was found according to the flood plain terrain. Subsequently, the water level of each individual cross section was derived from the elevation of the left and right border of the adjusted flood profiles. The same method was then conducted for the flood mask derived from the optical reference imagery. A comparison of the water level altitude of both data sets and each cross section is displayed in Fig. 6.

In contrast to the Elbe case study, further processing was applied to the flood profiles derived from TerraSAR-X data to estimate flood depth. Figure 7 presents the sequence

of the water level elevation of each flood profile in flow direction, showing a total vertical variation of about 2.7 m. Reasons for this are presumably residual classification errors and errors in the elevation model. The latter occur when the elevation model represents the vegetation surface instead of ground surface elevation.

The derived water levels were smoothed by applying a moving average filter. The smoothed water levels (shown in Fig. 7) represent the longitudinal water surface and serve as reference elevation for the flood depth computation. By applying the profile matching algorithm for the estimation of flood depth, all individual flood profiles were trimmed or extended according to their respective reference elevation. This means that all flood profiles were increased or decreased in their horizontal extent until their intersection point with the local flood plain terrain was found. The coordinates of the resulting left and right border of the matched flood profiles were then used together with the reference elevation to create a water surface triangulated irregular network (TIN). A continuous flood surface elevation was derived through TIN-interpolation. As the final step to obtain inundation depth, the DEM altitude was subtracted from the rasterised TIN. The result is illustrated in Fig. 8.

4.4 Results

Figure 8 indicates that the TerraSAR-X derived flood mask corresponds well to the flood mask derived from the optical reference imagery. In Fig. 6, a significant difference of 3–4 m in the elevation of the flood level compared to the mean water level of the River Severn can be recognised for all profiles. By averaging the flood water level via a moving window along the longitudinal profile (Fig. 7), discontinuities in the elevation of the flood surface and thus flood depth were minimised. However, the hydraulic situation shown in Fig. 7 is not as it would be usually expected in a hydraulic sense. Increasing water level from the mid-section of the longitudinal profile in downstream direction could have several individual causes or could be a combination of them. On the one hand, assuming that this is not due to inaccuracies in the DEM, a possible explanation is that the flood situation was recorded between two flood waves. On the other hand, a

possible levee breach in the middle part of the river reach would induce water flow into lower regions aside of the river channel. A third possible explanation would be a tidal flood wave from the nearby sea, blocking the downstream river flow.

As shown in Fig. 8, the created flood surface area from flood depth delineation corresponds to the flood mask derived from the aerial photograph. In comparison to the original flood mask, a significant improvement could be achieved regarding its consistency with the high resolution elevation model. That means that elevated objects inside the flood mask such as bridges and buildings or higher ground are automatically excluded.

5 Conclusions

Discussion of Results and Conclusion It could be demonstrated that for the given situation of the Elbe case study, a medium resolution SAR sensor such as Radarsat-1 significantly underestimated the flood extent. Generally, wind, water turbulence, shallow water over agricultural fields and areas covered with vegetation are responsible for high backscatter values in SAR data and thus often lead to a misclassification and underestimation of flooded areas. X-Band sensors such as TerraSAR-X working with short wavelengths are even more sensitive to wind and roughness on water surfaces (Horritt et al., 2003).

Also the geometric resolution has a substantial influence on classification accuracy and flood mask derivation. For medium resolution SAR instruments with a ground resolution of 10–15 m, a small amount of scatterers such as a single tree within a ground resolution cell that is predominantly covered by surface water, leads to a high backscatter value of the concerned pixel. Hence, the pixel is misclassified as “non-flooded”. This is especially the case for riparian vegetation at the land-water boundary which leads to an underestimation of the flooded area. Consequently, the land water boundary is not captured sufficiently which means that the flood level cannot be determined reliably.

With regard to scale it can be stated that the accuracy of the approach highly de-

pends on the quality and resolution of the DEM. However, also the relation of remote sensing data and DEM regarding their geometric resolution and quality are of importance. Ideally, both datasets should have a high resolution, with the DEM resolution being higher than the resolution of the remote sensing data. However, it could be demonstrated, that with a very high resolution 1 m LiDAR DEM combined with a medium resolution Radarsat-1 flood mask, the potential of the approach could not be fully exploited.

It can be concluded from this study that the profile matching method can generally be applied on different scales. For both cases presented, the profile method yielded better results with respect to accuracy and hydraulic plausibility of the flood masks compared to the uncorrected data sets. For high resolution SAR data in combination with very high resolution elevation data the proposed methodology allows the generation of reliable and hydraulically sound maps of inundation depth.

The presented approach is limited to basins with pronounced terrain and is not regarded as suitable for flat and extensive flood plains. The proposed method has not yet been applied in real-time flood mapping operations, but is expected to improve accuracy and hydraulic reliability of SAR-based flood monitoring applications significantly. Urban areas were excluded from this study because of limitations of SAR-based flood classification in flooded settlements. However, the method has to be tested for such flood situations. Assuming that the flood line can be reliably deduced for at least one river bank, a very precise potential flood mask can be provided for urban areas without consideration of levees or mobile flood barriers. Besides, the higher resolution SpotLight mode of TerraSAR-X can provide a benefit in water detection in these build-up areas.

The main drawback of the profile method is that its application is limited by the availability of high resolution digital elevation models which are rather expensive and not readily available for a large number of basins. However, during the last years LiDAR DEMs became more and more available and have been successfully used for hydraulic applications in river flood plains. In the near future, the upcoming TanDEM-X satellite

constellation renders the possibility to provide elevation data of a new dimension on a global scale (Krieger et al., 2005). On this basis the proposed method is a promising tool for improving flood monitoring and flood mapping, especially in very large ungauged basins.

Acknowledgements. This work was supported by the Helmholtz Association of German Research Centres and the German Aerospace Center (DLR) within the framework of the "DISFLOOD" Project. The authors wish to thank the Environment Agency of the United Kingdom for providing the LiDAR DEM and aerial photography of the Tewksbury region. Special thanks go to André Twele for supporting the flood depth computations and reading the manuscript, Alexandra Förster for reading the manuscript, Sandro Martinis for providing the TerraSAR-X flood mask and Marianne Wargenau for digitising the flood mask from aerial photos.

References

Baatz, M. and Schäpe, A.: Multiresolution Segmentation–an optimization approach for high quality multi-scale image segmentation, Angewandte Geographische Informationsverarbeitung XII. Beiträge zum AGIT-Symposium Salzburg, 200, 12–23, 2000.

Bates, P. D., Wilson, M. D., Horritt, M. S., Mason, D. C., Holden, N., and Currie, A.: Reach scale floodplain inundation dynamics observed using airborne synthetic aperture radar imagery: Data analysis and modeling, J. Hydrol., 328, 306–318, 2006.

Blaschke, T., Lang, S., Lorup, E., Strobl, J., and Zeil, P.: Object-oriented image processing in an integrated GIS/remote sensing environment and perspectives for environmental applications, in: Environmental Information for Planning, Politics and the Public, edited by: Cremers, A. and Greve, K.: Metropolis Verlag, Marburg, Germany, 2, 555–570, 2000.

Brivio, P. A., Colombo, R., Maggi, M., and Tomasoni, R.: Integration of remote sensing data and GIS for accurate mapping of flooded areas, Int. J. Remote Sens., 23, 429–441, 2002.

Fowler, R. A.: LIDAR for Flood Mapping, Earth Observation Magazine, 9, 2002, http://www.eomonline.com/Common/Archives/July00/robert.htm, access: 25 August, 2008.

Horritt, M. S., Mason, D. C., Cobby, D. M., Davenport, I. J., and Bates, P. D.: Waterline mapping in flooded vegetation from airborne SAR imagery, Remote Sens. Environ., 85, 271–281, 2003.

Krieger, G., Fiedler, H., Hajnsek, I., Eineder, M., Werner, M., and Moreira, A.: TanDEM-X: mission concept and performance analysis, IEEE International Geoscience and Remote Sensing Symposium Proceedings, 2005 (IGARSS '05), 25–29 July 2005, Seoul, South Korea, 4890–4893, 2005.

Ling, F., Xiao, F., Du, Y., Xue, H. P., and Ren, X. Y.: Waterline mapping at the subpixel scale from remote sensing imagery with high-resolution digital elevation models, Int. J. Remote Sens., 29, 1809–1815, 2008.

Matgen, P., Schumann, G., Henry, J. B., Hoffmann, L., and Pfister, L.: Integration of SAR-derived river inundation areas, high-precision topographic data and a river flow model toward near real-time flood management, Int. J. Appl. Earth Obs., 9, 247–263, 2007.

Meinel, G., Schumacher, U., and Hennersdorf, J.: GIS-Technical Evaluation of the Flood Disaster in Summer 2002 with respect to the City of Dresden on the Basis of Remote Sensing, Laser Scanner and Measurement Data, ISPRS International Archives of the Photogrammetry, Remote Sensing and Spatial Information Sciences, XXXIV, 104–111, 2003.

Sanders, B. F.: Evaluation of on-line DEMs for flood inundation modeling, Adv. Water Resour., 30, 1831–1843, 2007.

Sanyal, J. and Lu, X. X.: Application of Remote Sensing in Flood Management with Special Reference to Monsoon Asia: A Review, Nat. Hazards, 33, 283–301, 2004.

Schneiderhan, T., Huber, M., Zwenzner, H., and Hoffmann, J.: Use of ENVISAT ASAR and ERS SAR data for flood rapid mapping, ENVISAT Symposium, Montreux, Swiss, 2007.

Schumann, G., Hostache, R., Puech, C., Hoffmann, L., Matgen, P., Pappenberger, F., and Pfister, L.: High-Resolution 3-D Flood Information From Radar Imagery for Flood Hazard Management, IEEE T. Geosci. Remote, 45, 1715–1725, 2007.

Thieken, A. H., Müller, M., Kreibich, H., and Merz, B.: Flood damage and influenceing factors: New insights from the August 2002 flood in Germany, Water Resour. Res., 41, 1–16, 2005.

Wang, Y.: Seasonal change in the extent of inundation on floodplains detected by JERS-1 Synthetic Aperture Radar data, Int. J. Remote Sens., 25, 2497–2508, 2004.

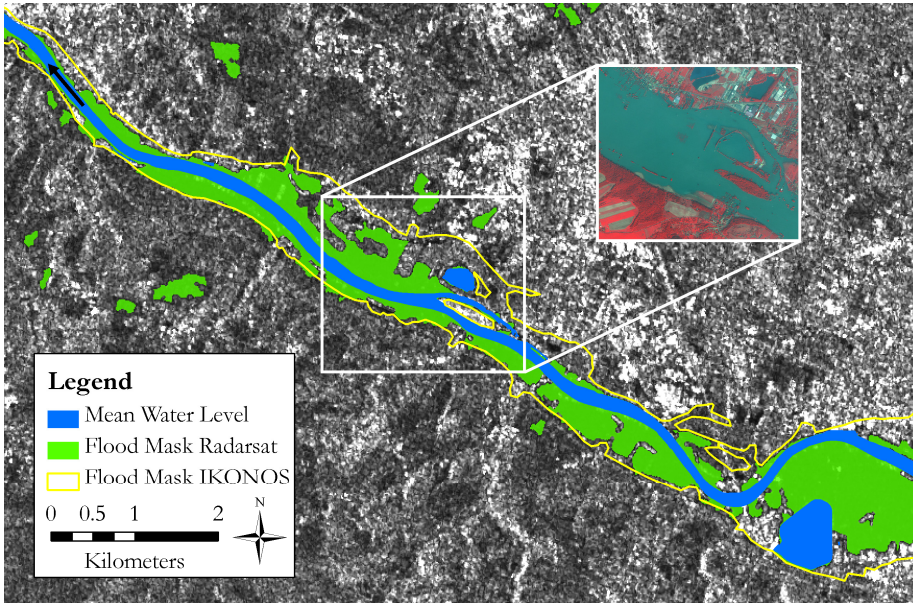

Fig. 1. Radarsat-1 image showing the flood situation of the Elbe River 15 km north-west of Dresden (Germany) on 18 August 2002, one day after the flood peak. For comparison a small subset of an IKONOS false colour image is presented which was acquired five hours after the Radarsat-1 scene.

HESSD
5, 2951–2973, 2008

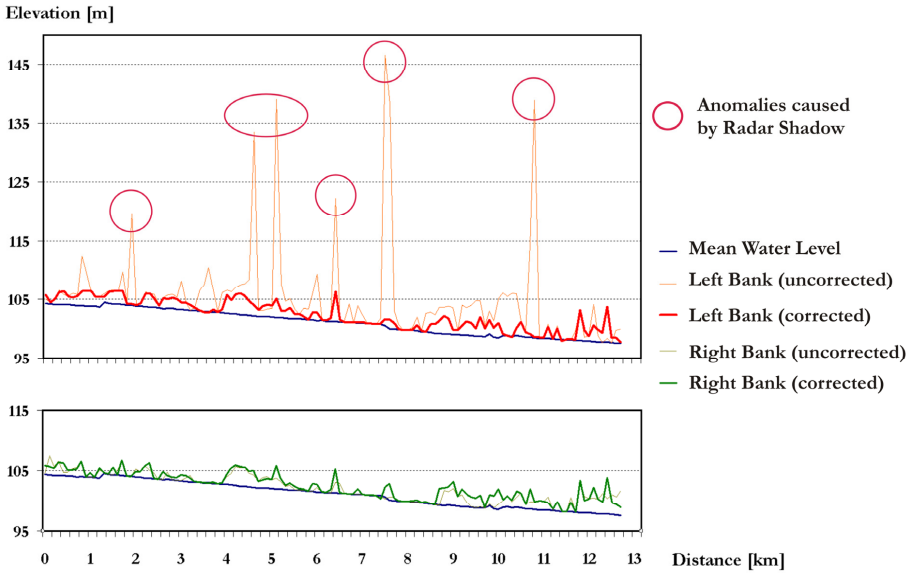

Fig. 2. Longitudinal profile showing the elevation of the left and right river bank at each individual Radarsat-1 profile before and after the rectification. Large anomalies can be recognised in the uncorrected elevation readings of the left river bank caused by misclassification of water due to radar shadow. After the horizontal adjustment (shifting) of the profile, elevation readings of the left and right river bank correspond to each other.

HESSD
5, 2951–2973, 2008

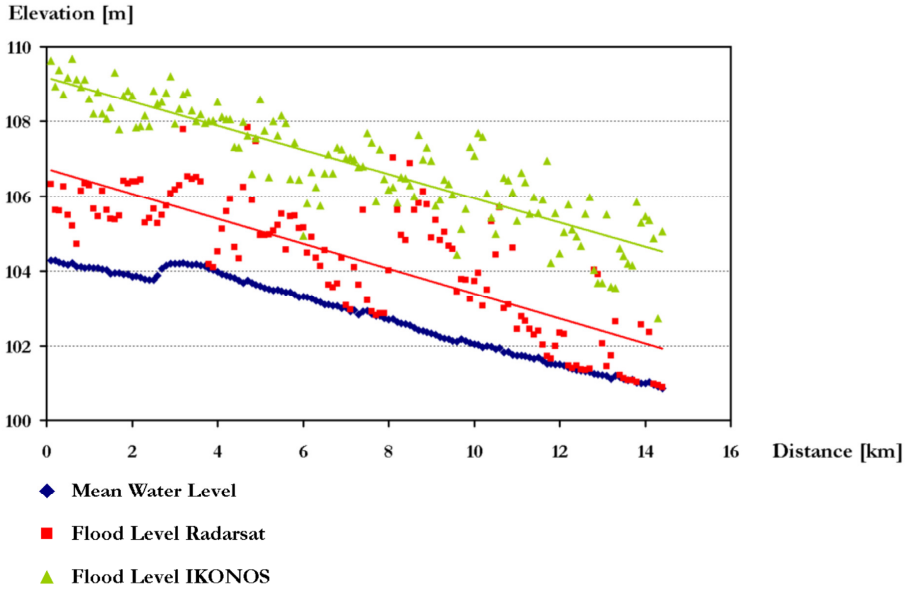

Fig. 3. Longitudinal profile of the Elbe River reach north-west of Dresden showing the elevation of the water level for each individual cross-section profile for Radarsat-1 (red) and IKONOS (green) in comparison to the normal water level (blue).

HESSD
5, 2951–2973, 2008

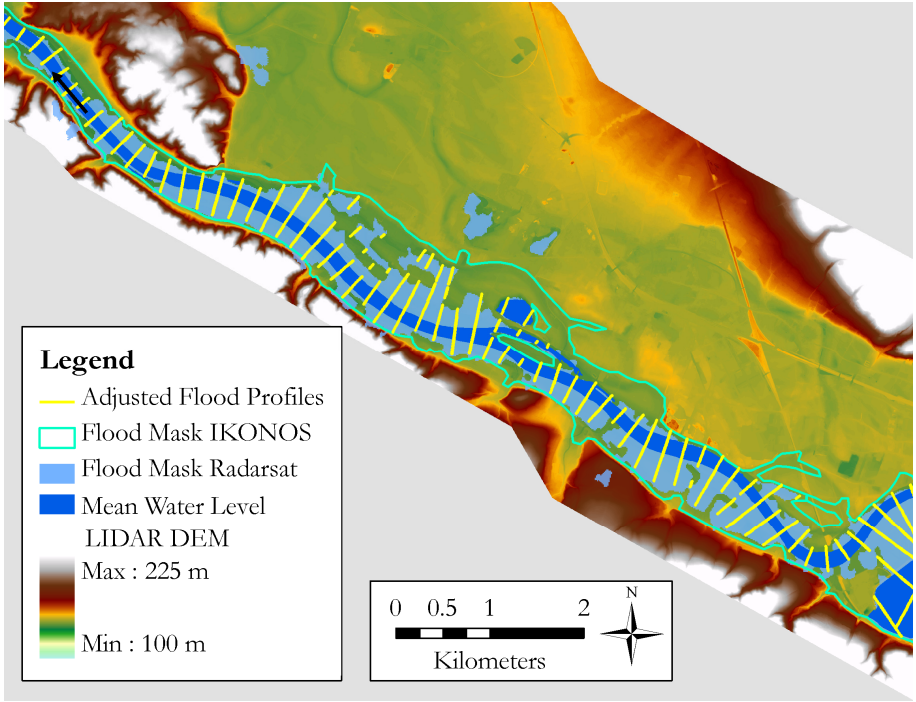

Fig. 4. Elevation map of the Elbe River north-west of Dresden with the original flood mask derived from Radarsat-1 (light blue). The cross section flood profiles which were horizontally shifted according to the LiDAR DEM present a plausibility check for each section of the flood mask. For comparison the flood mask derived from IKONOS is shown in lime-green colour.

HESSD
5, 2951–2973, 2008

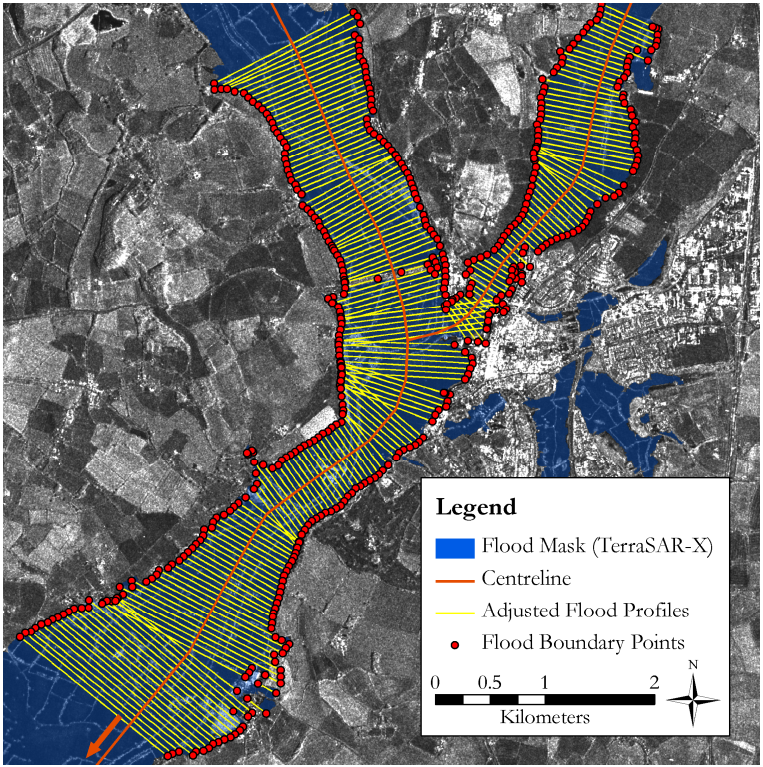

Fig. 5. TerraSAR-X image from 25 July 2007 showing the large flood event of the River Severn at Tewkesbury (UK). Cross section profiles with a distance of 50 m were created perpendicular to the flood centreline and were horizontally shifted according to the underlying high resolution elevation model. From the left and right boundary points the elevation of the water level could then be derived for each profile.

HESSD
5, 2951–2973, 2008

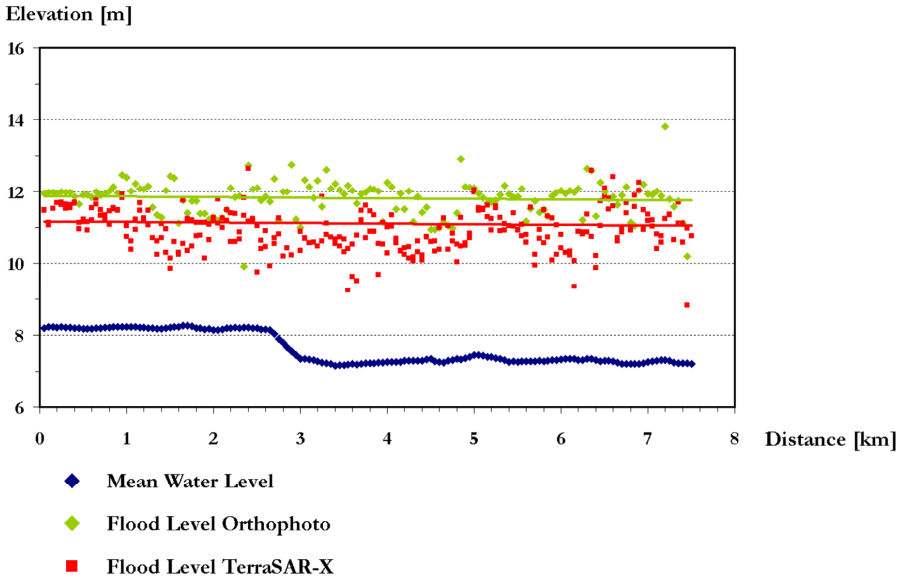

Fig. 6. Longitudinal profile showing the elevation of the water level for each individual cross-section profile derived from TerraSAR-X (red) and from an Aerial Photography survey (green) one day prior to the satellite overpass in comparison to the normal water level (blue).

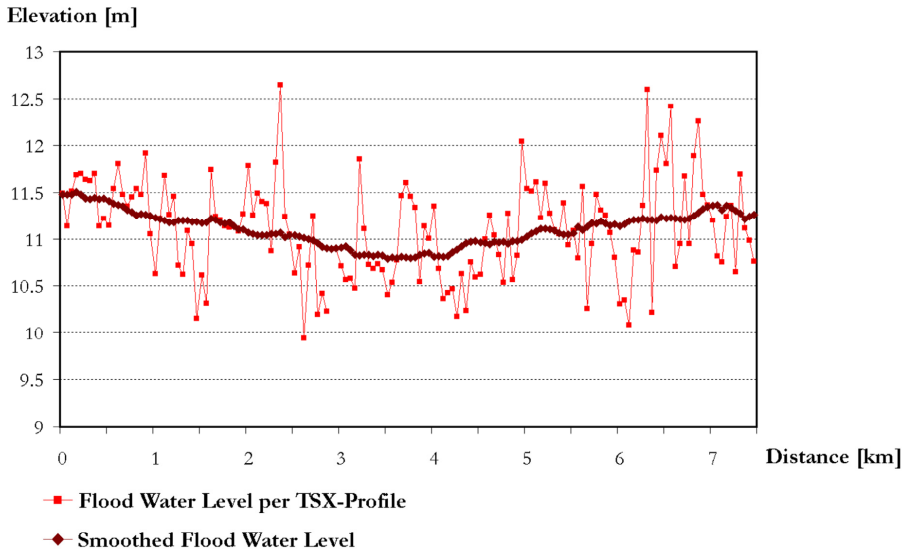

Fig. 7. Longitudinal Profile of the river reach showing the water level of the individual flood profiles derived from the TerraSAR-X flood mask. The water levels were smoothed by a moving average in order to diminish classification errors and possible inaccuracies in the elevation model. The smoothed line serves as reference flood level for the flood depth delineation.

HESSD
5, 2951–2973, 2008

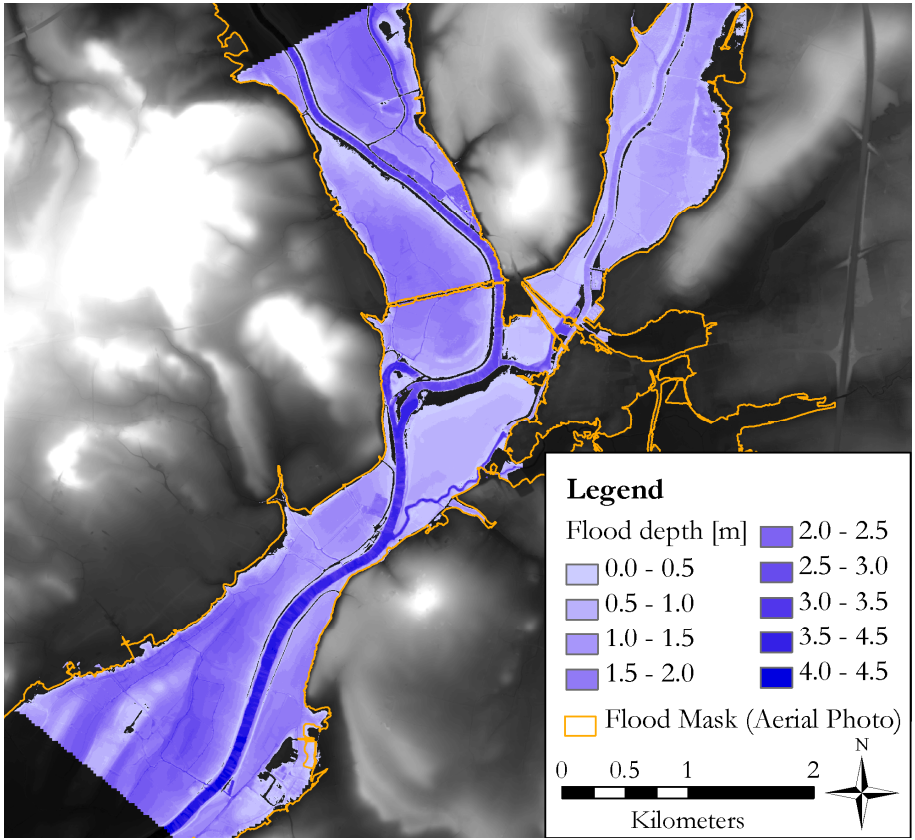

Fig. 8. Flood depth map of the River Severn near Tewkesbury derived from the rectified flood profiles of TerraSAR-X and a high resolution LiDAR elevation model. For comparison the flood extent derived from an aerial photography survey is shown by the yellow line. The urban area east of the river confluence was excluded from this study since the profile method was only applied along the river course.